Sixth International Symposium on Turbulence and Shear Flow Phenomena
Seoul, Korea, 22-24 June 2009

EXPERIMENTAL INVESTIGATION OF LORENTZ-FORCE CONTROLLED FLAT-PLATE BOUNDARY LAYER WITH LASER-DOPPLER VELOCITY-PROFILE SENSOR AND PARTICLE IMAGE VELOCIMETRY

Katsuaki Shirai, Andreas Voigt, Mathias Neumann, Lars Büttner, Jürgen Czarske
Technische Universität Dresden,
Chair of Measurement and Testing Techniques
Helmholtzstraße 18, D01069, Dresden, Germany
katsuaki.shirai@tu-dresden.de

Christian Cierpka*, Tom Weier, Gunter Gerbeth
Forschungszentrum Dresden-Rossendorf,
Magnetohydrodynamics Division
Bautzner Landstraße 128, D01328, Dresden, Germany

ABSTRACT

A study was made on electrically conducting flow over a flat plate boundary layer controlled with streamwise stationary Lorentz forces. Two different velocity measurement methods were used for the experimental investigation: laser Doppler velocity profile sensor and time resolved particle image velocimetry. The flow measurements were mainly focused on the near-wall behaviors of the flow with different magnitudes of the Lorentz forces. Velocity distributions and local acceleration were evaluated from the experiments. The experimental results revealed that the near-wall fluid is accelerated due to the streamwise Lorentz force and the turbulence fluctuation is suppressed by the increase of the Lorentz force applied. The limitations of the experiments and the future perspectives on the investigation are addressed.

INTRODUCTION

Lorentz, i.e. electromagnetic, forces may be used to influence a flow, if the fluid is electrically conducting. This possibility is meanwhile routinely used in the case of liquid metals and semiconductor melts, where conductivities are high and other methods of flow control are not readily available. For low conducting fluids such as electrolytes like seawater, Lorentz force based flow control is less common, but has received some attention during the last years. A major problem for applications is in this case the low energetical efficiency. It is basically caused by the low conductivity of the fluid. Shatrov and Gerbeth (2007) provide a detailed discussion of the nature of the efficiency deficit. Despite this low energetical efficiency, Lorentz force actuators remain of interest for basic research in flow control since they possess several distinct features: momentum is directly generated in the fluid without associated mass flux, the frequency response of the actuation is practically unlimited, no moving parts are involved.

First investigations of the electromagnetic control of electrolyte flows date back to the 1950's. Already in 1954, Crausse and Cachon provided experimental evidence of successful separation postponement as well as separation provocation on a half cylinder. Rossow (1957) and Resler and Sears (1958) discussed aerospace applications in ionized air, among other things, to control heat transfer to reentry vehicles. A few investigations on laminar flow control (e.g. Gailitis and Lielausis, 1961) and related topics have been published later on, but the activities declined with the beginning 1970's. A renewed interest in electromagnetic flow control for low conducting fluids arose in the 1990's. The majority of papers dealt with skin friction reduction of turbulent boundary layers. For this purpose, different force configurations have been investigated. Nosenchuck and Brown (1993), Rossi and Thibault (2002) and others used nominally wall normal, time dependent forces. However, the real force distribution produced by the electromagnetic tiles is quite complex and may play a crucial role (Rossi and Thibault, 2002). Wall parallel forces in streamwise direction have been applied, e.g., in the experiments of Henoch and Stace (1995) and Weier et al. (2001). This force configuration increases wall shear stress, because the acceleration of the near wall fluid leads to a higher slope of the mean velocity profile in streamwise direction. However, the momentum gain due to the Lorentz force surpasses the friction drag rise. Time dependent wall parallel forces in spanwise direction have been investigated numerically by, among others, Berger et al. (2000), and experimentally by and Breuer et al. (2004). Drag reductions ranging from 10% for the directly measured mean drag coefficient (Breuer et al., 2004) to 40% for the local skin friction (Pang and Choi, 2004) have been found, indicating that this type of forcing is indeed able to reduce skin friction drag of turbulent flows. Nevertheless, the energy balance of the approach is not favorable.

Particle image velocimetry (PIV) has been extensively used to investigate separated flows under instationary electromagnetic excitation (e.g., Weier et al., 2004; 2007). However, the high spatial resolution desirable in boundary layers can not be achieved with the PIV equipment available to the authors. In addition, the relative measurement error of PIV is estimated to be around 1% (Tropea et al., 2007), which may generate increased (artificial) turbulence levels in a nominally laminar flow.

Therefore, it is desired to use an alternative measurement technique in addition to PIV. The technique should be able to evaluate low turbulence degrees in the near-wall region even at strong Lorentz forces with bubbly conditions.

*Now at Universität der Bundeswehr München, Germany

Because of the near-wall region and electrically conductive fluid, the use of electrical probes such as hot-film anemometry is not preferred and non-intrusive methods are desired. The use of laser Doppler velocimetry (LDV) can be a candidate since it is a non-intrusive technique with a high spatial resolution. However, LDV has to be applied in the near-wall region with its optical axis nearly parallel to the wall surface in order to maximize the spatial resolution in the wall-normal direction. This measurement configuration necessitates optical access from the side and the sending beams have to go all the way through the bubbly region when a strong Lorentz force is applied. The use of LDV through bubbly region is known to be challenging (Groen et al., 1999).

The laser Doppler velocity profile sensor developed at the TU Dresden is attractive since it has a high spatial resolution down to sub-micrometers range and an accuracy of better than 0.1% in demanding flows. For instance, the sensor has been successfully applied to the near-wall region of a turbulent channel flow up to moderate Reynolds numbers (Shirai et al., 2008).

The purpose of the present investigation is to study the fundamental mechanisms of the flow control with Lorentz forces applied in electrically conductive fluid flows. For that reason, velocity distributions are measured both with the velocity profile sensor and the PIV especially with the emphasis on the near-wall regions. The streamwise and wall-normal velocity components are evaluated and their statistics are compared at different conditions of the applied Lorentz force. Furthermore, an attempt is made to evaluate the actuating force to the local fluid by the Lorentz forces.

THEORETICAL BACKGROUND

The principle of boundary layer control with Lorentz force is described in this section. A two-dimensional flow is considered as shown in Fig. 1 with x, y and z taken for the streamwise, the wall-normal and spanwise coordinate, respectively.

The Navier-Stokes equation becomes

$$\frac{\partial \boldsymbol{u}}{\partial t} + (\boldsymbol{u}\cdot\nabla)\,\boldsymbol{u} = -\frac{1}{\rho}\nabla p + \nu\nabla^2\boldsymbol{u} + \boldsymbol{f}, \qquad (1)$$

with $\boldsymbol{u}=(u,v,w)^T$ being the velocity vector. The vector $\boldsymbol{f}$ indicates the body force acting in a unit volume ($\boldsymbol{F}=\rho\boldsymbol{f}$: external force). The parameters ρ and ν are the fluid density and kinematic viscosity, respectively. In the present study, the external body force $\boldsymbol{F}$ is electromagnetic force, i.e., Lorentz force generated by electric and magnetic fields.

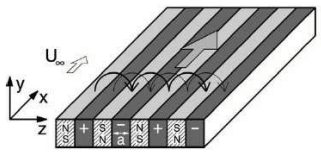

Figure 1: The concept of boundary layer control over a flat plate with wall-parallel Lorentz force (Weier et al., 2004)

.

The body force $\boldsymbol{F}$ is the vector product of the current density $\boldsymbol{j}$ and the magnetic induction $\boldsymbol{B}$

$$\boldsymbol{F} = \boldsymbol{j} \times \boldsymbol{B}, \qquad (2)$$

with $\boldsymbol{j}$ being provided by the Ohm's law

$$\boldsymbol{j} = \sigma\,(\boldsymbol{E} + \boldsymbol{u}\times\boldsymbol{B})\,. \qquad (3)$$

Here, $\boldsymbol{E}$ denotes the electric field vector and σ the electrical conductivity. Consequently, the Lorentz force due to these currents becomes negligible and it is necessary to apply an electric field of magnitude with $E_0 \gg U_0 B_0$ (U_0: velocity magnitude, B_0: magnitude of magnetic induction). This implies that the force distribution can be determined independently of the flow field by applying sufficiently large electric fields. In the present study, stationary application of wall-parallel Lorentz force in the streamwise direction is considered in order to see the fundamental behaviors of fluid in the near-wall region under control.

FLOW APPARATUS

The flow apparatus consists of a closed-circuit channel flow with open surface and a specially-made flat plate with electrodes and magnets embedded inside. The facility is located in the MHD division of the FZD in Rossendorf near Dresden in Germany.

The channel flow is operated with a constant water head for maintaining the constant flow velocity. The channel was mainly made out of polyvinyl chloride, polymethyl methacrylate (PMMA, Plexiglass) and stainless steel to avoid possible corrosion problems caused by the working fluid. The dimensions of the test section are $1\times0.2\times0.2$ m^3. It was preceded by a two-dimensional contraction with a ratio of 3:1. Two layers of plastic honeycombs and several layers of metal wire mesh with different mesh sizes were installed upstream of the contraction in order to break possibly existing large scale structures upstream. In addition, a sheet of filter pad was mounted for filtering out impurities from the electrolyte solution. The liquid which flew through the channel was collected into a basin and was recirculated by a pump. The channel was designed to have a constant free stream velocity of about U_∞=0.1 m/s. The working fluid was 0.25 molar NaOH electrolyte solution with a weak electrical conductivity in the fluid.

The flat plate was specially fabricated with metal and its nose was made with a super-ellipsoidal shape for avoiding flow separation at the leading edge. The surface of the plate was covered with stripes of permanent magnets and electrodes embedded inside in order to generate the actuating time continuous Lorentz force in the streamwise direction (see Fig. 1). The electrodes and magnets were both flush mounted in order not to disturb the flow over the plate. The width of each stripe was about 1 cm and the magnet and electrodes were installed alternatively with the full span of the plate. The plate was fixed in the channel parallel to the main flow direction. Both electric and magnetic fields possess only components in the wall-normal y and spanwise z directions, hence the resulting Lorentz force has only a streamwise (x) component $\boldsymbol{F_x}=F$. Near the plate surface, strong spanwise variations of the force density appear caused by singularities of the equations for both magnetic and electric fields exist, but these inhomogeneities rapidly decrease with increasing wall distance. Averaged over the spanwise direction, the mean force density shows an exponential decay with increasing wall distance (Weier et al., 2001)

$$F = \frac{\pi}{8} j_0 M_0 e^{-\frac{\pi}{a}y}, \qquad (4)$$

with M_0 being the magnetization of the permanent magnets and j_0 the applied current density σE_0, respectively. The magnetic induction in the wall-normal direction at the surface of the magnetic poles B_0 can be calculated from the geometry of the magnets and their magnetization M_0. In

the present configuration the electrodes and magnets have the same width a. The ratio of the electromagnetic force to the frictional force, i.e., modified Hartmann number Z can be written (Weier et al., 2001)

$$Z = \frac{1}{8\pi}\frac{j_0 M_0 a^2}{\rho\nu U_\infty}. \quad (5)$$

where a denotes the width of the electrodes. Experimental confirmation of the accelerating effect of the fluid has been reported in a flat plate boundary layer (Henoch and Stace, 1995; Weier et al., 2001). Depending on the force strength, even a distinct wall jet can be established. For Z=1, the growth of the boundary layer is inhibited. Assuming the Lorentz force density distribution to be uniform in the spanwise direction and exponentially decaying with the distance y from the wall, an exponential velocity profile is obtained for the streamwise velocity

$$\frac{u}{U_\infty} = 1 - e^{-\frac{\pi}{a}y}, \quad (6)$$

following a solution of the Navier-Stokes equation in a laminar boundary layer.

VELOCITY PROFILE SENSOR

The laser Doppler velocity profile sensor was proposed as an extension of conventional laser Doppler velocimetry for high spatially resolved measurements of local flow velocities (Czarske et al., 2001). It resolves both the axial positions and velocities of single tracer particles and hence the spatial distribution of velocities inside the measurement volume is reproduced without the need of being traversed.

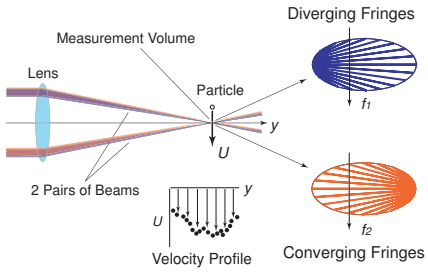

Figure 2: Schematic principle of a laser Doppler velocity profile sensor.

The basic principle of the velocity profile sensor is the use of a pair of fan-like fringe systems in the measurement volume as schematically shown in Fig. 2. Usually, a combination of divergent and convergent fringe systems is chosen for achieving a high spatial resolution in the optical axis. The quotient of the resulting Doppler frequencies from the two fringe systems becomes a unique function of the axial position inside the measurement volume, and hence the position y can be measured independently of the velocities as long as the fringe spacings are known in advance from calibration. The details of the working principle has been described in the past proceedings of the TSFP conference series (e.g., Shirai et al., 2005; 2007). As an extension, the sensor was further developed for the evaluation of axial velocity component (Büttner et al., 2006) and local flow accelerations (Bayer et al., 2008) based on time-frequency analysis of Doppler signal pairs.

The measurement head of the present sensor system was realized with a special design with fiber optics. The details of the sensor system are described in Pfister et al. (2005). The present sensor distinguishes the signals from the two channels based on different carrier frequencies. For the detection of signals, backward scatterings was mainly used and it was switched to sideward scattering in the region close to the wall. The sideward scattering was effective for measurements in the vicinity of the wall in order to avoid the strong reflection of the incident laser beam hitting at the wall. The sensor head was traversed several times due to the thick boundary layer. The traverse was monitored by a laser triangulation sensor with 1 μm precision. The sensor was calibrated with a small scattering object moving at a defined velocity in the same liquid used in the flow experiment. The sensor had a spatial resolution σ_y of about 118 μm in the direction of optical axis with the length of 1800 mm in the liquid. The lateral size of the measurement volume was estimated to be approximately 150 μm in the liquid. The relative uncertainty of velocity measurements was 0.32%. The position and velocity uncertainties are rather large compared to the sptaial resolution of 20 μm and the velocity uncertainty of 0.1% for the same sensor in air. This attributed to a number of reasons – the velocity stability of the pinhole used in the calibration, the increase of the measurement volume in the liquid due to the refracive index change and the noises in the electrical circuits. For tracer particles, silver-coated hollow-glass spheres with an averaged diameter of 10 μm were seeded in the flow.

PIV

The second set of flow measurements was performed with a PIV system. An Ar-ion laser beam was expanded into a light sheet and directed from the top to the measurement location vertical to the flat plate. In order to avoid instability of the light sheet due to the free surface of the liquid, a PMMA plate was installed, which provided a stable surface at the location of the light sheet. Vestosint particles with an averaged diameter of 25 μm were used as tracers. The measurement region was set to approximately 40×40 mm^2. A Photron high speed camera was used at 125 Hz to record images from the side. The magnification was 23.265 Px/mm. Using elongated windows with 32×16 Px^2 and an overlap of 50 % results in a resolution of 0.7×0.3 mm^2. The camera is equipped with 8 GB memory providing a storage capacity up to 11376 images, which leads to a measurement time of 91 seconds. The electrolyte bubbles rising out of focus had an intensity at least one order less magnitude compared to that of tracer particles. The gray film generated by the bubbles as well as wall reflections were eliminated using a high pass filter (6.5 Px). Nevertheless for the highest value of the current (Z=3.81) the signal to noise ratio (SNR) decreased dramatically. In this configuration a high pass filter (8 Px) was used, together with binarization (threshold 8) and Gaussian smoothing (3×3 Px^2) was applied. In addition, the window size was increased in the vertical direction to 24 Px. Averaging was performed in time (using only valid vectors from the PIV results) and in space (±11 profiles meaning ±7 mm in physical space). Calibration of the PIV system was performed in situ using a precision grid plate.

EXPERIMENTS

Series of flow measurements were carried out at a single streamwise location of the plate with the velocity profile sensor or the PIV system. The flat plate was installed so that the plate surface became parallel to the main flow direction. The measurement configuration of the flat plate was different for the measurements with the velocity profile

sensor (vertical) and for the PIV system (horizontal) due to the optical access of these two techniques. The measurement location and the freestream velocity were set as close as possible for the two measurement techniques. The measurements were performed with different conditions of the streamwise Lorentz forces. The conditions of the Lorentz force were Z=0, 1.05, 1.57 and 4.01 for the velocity profile sensor and Z=0, 1.49 and 3.81 for the PIV. A higher value of Hartmann number corresponds to stronger Lorentz force as can be seen from Eq.(5). The modified Hartmann numbers did not precisely match for the two measurement techniques because of slightly different freestream velocities. The case of Z=0 corresponds to the ordinary boundary layer without any control. The case of Z=1 corresponds to the exponential profile. At higher Hartmann numbers, electrolysis occurred and bubbles were generated on the electrodes with the applied electric current. These flow regimes are basically considered to be laminar since the Reynolds numbers were far below the critical one for transition to turbulence. The streamwise velocity u, wall-normal velocity v and streamwise acceleration a_x were measured with the velocity profile sensor. In the PIV measurement, streamwise and wall-normal velocities were measured.

Table 1: The slot width and number of samples in each slot for different parameters in the statistical calculation.

parameter	slot width [μm]	number of samples
velocity u	200	1100
velocity v	2800	14000
acceleration a_x	2000	10000

RESULTS

The exact location of the wall was determined with a series of linear fits for the streamwise velocity data without Lorentz force near the wall in the case of the velocity profile sensor. The wall position was determined with an uncertainty of $\pm$20 μm. The closest pointed to the wall measured was 75 μm away from the wall. The flow statistics were calculated with a slot technique with 50% overlapping of neighboring slots. The slot width was varied for different parameters depending on the statistical convergence and data scatter of rms values. The resulting optimum slot widths and the averaged numbers of samples contained in each slot are listed in Table. 1 for the respective parameters. An outlier reduction based on the norm of the point to the local linear fit in each slot was applied with a velocity bias correction. The number of samples discareded by the outlier reduction was typically less than 0.5% at each slot and at maximum a few percent for all the parameters.

Streamwise Velocity

The mean velocity distributions are plotted in Fig. 3(a) measured with the velocity profile sensor and with the PIV. The closed symbols are the results of the velocity profile sensor and the open ones are those of the PIV. The results are normalized with the corresponding freestream velocities without Lorentz force, and the wall-normal coordinate y was converted into similarity variable η defined as

$$\eta = y\sqrt{\frac{U_\infty}{\nu x_m}} \tag{7}$$

for Blasius solution. The parameters U_∞ and x_m are the freestream velocity and the distance of the measurement location from the leading edge, respectively. The traverse scales of the wall normal coordinate were corrected for the refractive index in the liquid. The measured velocity profiles clearly show the difference with the applied Lorentz force. The results of the both two measurement techniques have reasonable agreements, however, there are systematic difference between their results. This may have been caused by the different measurement configurations for the velocity profile sensor and the PIV, although the experiments were carefully performed for setting the identical conditions. The mean velocity without Lorentz force (Z=0) traces very well the feature of the theoretical profile of the Blasius solution. The velocity profile with Lorentz force shows increased, which indicates the fluid is accelerated by the application of the streamwise Lorentz force as can be anticipated. The results of the velocity profile sensor show some velocity increases near the wall for the conditions with the streamwise Lorentz force application. This was likely due to the bubbles created by the electrolysis.

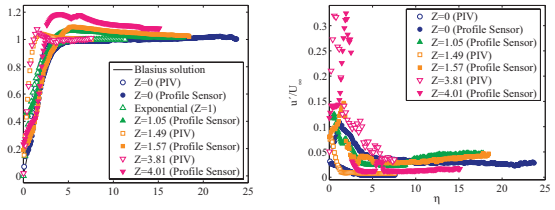

Figure 3: Normalized streamwise velocity statistics at different Lorentz force conditions, (a) mean velocity (left), (b) rms velocity (right). (Z: modified Hartmann number)

The rms velocity profiles in the streamwise direction are shown in Fig. 3(b) normalized in the same way as for the mean velocity profile. They show very similar features to those measured with the PIV, which demonstrates the justification of the two experimental methods for this flow investigation. They show a peak close to the wall and the peak height increases with the magnitude of the Lorentz force applied. This peak corresponds to the increase of the velocity gradient in the mean velocity with the Lorentz force (see Fig. 3(a)). Away from the wall, the fluctuating velocity decreases with the magnitude of the Lorentz force. The Lorentz force worked for reducing the streamwise turbulence fluctuation while accelerating the velocity near the wall. The velocity fluctuations measured with the profile sensor are consistently larger than those of the PIV data, which was unexpected. This attributed to the flow disturbance caused by the blockage effect with the sideward detection optics immersed in the liquid in order to achieve velocity measurements very close to the wall with the velocity profile sensor.

Wall-Normal Velocity

Normalized wall-normal velocity distributions are shown in Fig. 4. A different normalization was applied to the wall-normal velocity results compared to the streamwise ones. For comparison, the wall-normal velocity distribution from the Blasius solution is shown for the case of Z=0 in Fig. 4(a). The theoretical distribution exhibits positive values, but neither the velocity profile sensor nor the PIV could capture this theoretical behavior. The wall-normal velocities measured with the profile sensor is consistently larger in magnitude than those with the PIV (see Fig. 4(b)). This was supposed to be caused by the large measurement uncertainty for the wall-normal velocity with the velocity profile sensor (Büttner and Czarske, 2006). Nevertheless, the results show

that there was a consistent flow toward the wall and the velocity magnitude increases away from the wall as well as with the Lorentz force. This is natural because if the flow was accelerated in the streamwise direction near the wall, fluid has to be supplied into near-wall region from outside the boundary layer. The Fig. 4(b) shows that the fluctuation of the wall-normal velocities increases near the wall with the magnitude of the Lorentz force. The results of the PIV shows consistently higher values than those with the velocity profile sensor.

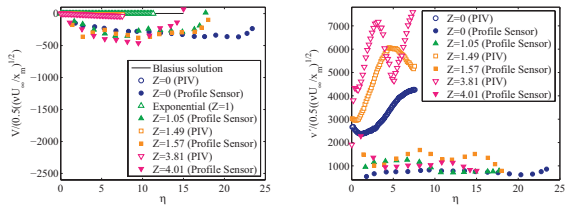

Figure 4: Normalized wall-normal velocity statistics at different Lorentz force conditions, (a) mean velocity (left), (b) rms velocity (right).

Streamwise Acceleration

Normalized streamwise acceleration distributions are shown in Fig. 5. The acceleration data are available only for the velocity profile sensor. The theoretical distribution of the streamwise acceleration derived from Blasius solution is shown together. The theoretical distribution exhibits a small negative peak around η=2.9. The measured mean accelerations show consistently negative values but are about two orders of magnitude larger than the theoretically estimated values (see Fig. 5(a)). One might expect positive acceleration since the fluid is accelerated in the near-wall region. However, the acceleration term exhibits an opposite behavior as explained in the next section.

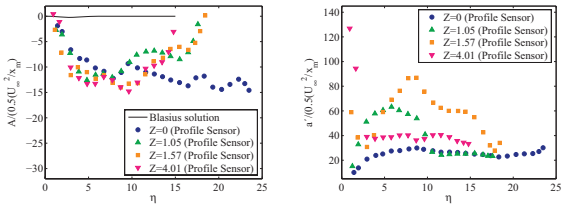

Figure 5: Normalized streamwise acceleration statistics at different Lorentz force conditions, (a) mean acceleration (left), (b) acceleration rms (right).

DISCUSSIONS

The velocity distributions measured with the two different measurement methods revealed the influence of the stationary streamwise Lorentz force over the flat plate boundary layer in the electrically conductive fluid flow. Due to the Lorentz force, fluid near the wall is accelerated and the flow velocities exhibit similar behaviors to wall jets. The measurement results indicate that the fluid away from the wall entrains into the near-wall accelerating flow due to the Lorentz force.

The measured acceleration showed negative values although the fluid near the wall is accelerated by the Lorentz force. The origin of the negative acceleration values can be explained by checking the material derivative terms in the Navier-Stokes equation. The material derivative (i.e., local fluid acceleration) consists of three terms for the streamwise direction with the assumption of two-dimensional flow

$$a_x = \frac{Du}{Dt} = \frac{\partial u}{\partial t} + u\frac{\partial u}{\partial x} + v\frac{\partial u}{\partial y}. \quad (8)$$

In the present case, the flow is temporally steady and hence the temporal acceleration is considered to be zero. Then, the spatial derivative of the streamwise velocity in the streamwise direction should be positive while its wall-normal derivative has a certain positive value with the wall-normal velocity being negative. Therefore, the streamwise acceleration can be negative due to the negative wall-normal velocity together with the velocity gradient. The streamwise Lorentz force increases the velocity gradient and induced a wall-jet like flow, which increases the entrainment of the fluid from the outside of the boundary layer. Therefore, the acceleration term is expected to have larger magnitudes with the Lorentz force. The measured acceleration distribution needs to be carefully interpreted. The measurement uncertainty of the acceleration is rather large in the range of 50 with the non-dimensional values. The minimum measurable non-dimensional acceleration magnitude is actually a function of the incident velocity for the velocity profile sensor (Bayer et al., 2008). Theoretically estimated minimum measurable acceleration becomes approximately $44((1/2)U_\infty^2/x_m)^2$, which yields 44 at the freestream velocity condition matching well with the rms values of the streamwise accelerations in Fig. 5(b). This rather large uncertainty hinders reliable evaluation of the acceleration in the present results. Therefore, the evaluation of the actual controlling force becomes difficult.

The second purpose of the present investigation to evaluate the small degree of turbulence fluctuations was not achieved with the expense of the measurements very close to the wall. The closest point measured in the previous experiment was around 500 μm with the same sensor using only a backward scattering detection while it was 75 μm using the sideward scatter detection this time. This was an advance when the average size of the tracer particles (10 μm) is considered. However, the sideward detection optics immersed into the flow may have induced local flow disturbances. This was partly due to the flow apparatus with a free surface of liquid. A flow without free liquid surface (i.e., internal flow) with a proper optical access would be promising except for the evacuation issue of hydrogen bubbles generated by the electrolysis with the Lorentz forces.

The examination of pure influence of the Lorentz force is indeed complicated due to the bubbles generated by the electrolysis when Lorentz forces above a certain magnitude are applied. The bubbles might have made not only the evaluation of the signals difficult but could also influence the flow structures by some interactions. The bubbles may have interacted with the electromagnetic field. For instance, small bubbles have been known to contribute on drag reduction in turbulence boundary layers by Deutsch and coworkers (e.g., Madavan et al., 1984). Hence, further experiments may be required to make concrete statements on the evaluation of the influences originating from the Lorentz forces alone. For that purpose, one could use liquid with a higher electrical conductivity generating less bubbles such as liquid metals. However, optical measurement techniques are not applicable any more when liquid metal is used. An alternative is to conduct a series of experiments with controlled bubble void fraction conditions to separate the influences of Lorentz force and electrolyte bubbles. However, the independence of these influences may not be guaranteed – the

Lorentz force field and the bubbles may interact to modify the flow structure. Therefore, fundamental investigations of bubbles and surrounding fluid behaviors under electromagnetic forces are of essential importance.

SUMMARY AND OUTLOOK

The flow behaviors in a boundary layer over the flat plate controlled with streamwise stationary Lorentz force were investigated with two different optical measurement methods. The velocity distributions were successfully measured with the fiber-optic laser Doppler velocity profile sensor and the PIV down to the vicinity of the wall, where the electrodes and magnets integrated. The streamwise and wall-normal velocities and the streamwise acceleration were evaluated. The measurement results revealed the fluid acceleration near the wall due to the applications of the Lorentz force. The streamwise velocity exhibits wall-jet like behavior near the wall with the increase of the magnitude of the Lorentz force. Further investigations could provide more insights on the complex interactions of the Lorentz force and the resulting electrolyte bubbles in electrically weak conductive fluids in boundary layers.

ACKNOWLEDGEMENTS

The German Research Foundation (DFG) is gratefully acknowledged for supporting the present work in the framework of the Collaborative Research Centre 609 "Electromagnetic Flow Control in Metallurgy, Crystal-Growth and Electro-Chemistry".

REFERENCES

Bayer, C., Shirai, K., Büttner, L., and Czarske, J., 2008, "Measurement of acceleration and multiple velocity components using a laser Doppler velocity profile sensor", *Meas. Sci. Technol.*, Vol. 19, 055401 (11pp).

Berger, T.W., Kim, J., Lee, C., and Lim, J., 2000, "Turbulent boundary layer control utilizing the Lorentz force", *Phys. Fluids*, Vol. 12, pp. 631-649.

Breuer, K., Park, J., and Henoch, C., 2004, "Actuation and control of a turbulent channel flow using Lorentz forces", *Phys. Fluids*, Vol. 16, pp. 897-907.

Büttner, L., and Czarske, J., 2006, "Determination of the axial velocity component by a laser-Doppler velocity profile sensor", *J. Opt. Soc. Am. A*, Vol. 23, pp. 444-454.

Crausse, É., and Cachon, P., 1954, "Actions électromagnétiques sur les liquides en mouvement, notamment dans la couche limite d'obstacle immergés", *CRAS*, Vol. 238, pp. 2488-2490.

Czarske, J., Büttner, L., Razik, T., and Welling, H., 2001, "Measurement of velocity gradients in boundary layers by a spatially resolving laser Doppler sensor", *Proc. SPIE: Optical Diagnostics for Fluids, Solids, and Combustion*, Vol. 4448, pp. 60-71.

Czarske, J. Büttner, L., Razik, T., and Müller, H., 2002, "Boundary layer velocity measurements by a laser Doppler profile sensor with micrometre spatial resolution", *Meas. Sci. Technol.*, Vol. 13, pp. 1979-1989.

Gailitis, A., and Lielausis, O., 1961, "On a possibility to reduce the hydrodynamic resistance of a plate in an electrolyte", *Appl. Magnetohydrodynamics, Rep. Phys. Inst.*, Vol. 12, pp. 143-146.

Groen, J.S., Mudde, R.F., and Van Den Akker, H.E.A., 1999, "On the application of LDA to bubbly flow in the wobbling regime", *Exp. Fluids*, Vol. 27, pp. 435-449.

Henoch, C., and Stace, J., 1995, "Experimental investigation of a salt water turbulent boundary layer modified by an applied streamwise magnetohydrodynamic body force", *Phys. Fluids*, Vol. 7, pp. 1371-1383.

Madavan, N.K., Deutsch, S., and Merkle, C.L., 1984, "Reduction of Turbulent Skin Friction By Microbubbles", Phys. Fluids, Vol. 27, pp. 356-363.

Nosenchuck, D., and Brown, G., 1993, "Discrete spatial control of wall shear stress in a turbulent boundary layer", *Near-Wall Turbulent Flows, R. So, G. Speziale, B. Launder eds., Elsevier*, pp. 689-698.

Pang, J., and Choi, K.S. (2004), "Turbulent drag reduction by Lorentz force oscillation", *Phys. Fluids*, Vol. 16, pp. L35-L38.

Pfister, T., Büttner, L., Shirai, K., and Czarske, J., 2005, "Monochromatic heterodyne fiber-optic profile sensor for spatially resolved velocity measurements with frequency division multiplexing", *Appl. Optics*, Vol. 44, pp. 2501-2510.

Resler, E.L., Jr, and Sears, W.R., 1958, "The prospects for magneto-aerodynamics", *J. Aero. Sci.*, Vol. 25, pp. 235-245, 258.

Rossi, L, and Thibault, J.P., 2002, "Investigation of wall normal electromagnetic actuator for seawater flow control", *J. Turbulence*, Vol. 3, no. 005.

Rossow, V.J., 1957, "On flow of electrically conducting fluids over a flat plate in the presence of a transverse magnetic field", *NACA TN 3971.*

Shatrov, V., and Gerbeth, G., 2007, "Magnetohydrodynamic drag reduction and its efficiency", *Phys. Fluids*, Vol. 19, 035109 (12pp).

Shirai, K., Bayer, C. Voigt, A., Pfister, T., Büttner, L., and Czarske, J., 2008, "Near-wall measurements of turbulence statistics in a fully developed channel flow with a novel laser Doppler velocity profile sensor", *Euro. J. Mech., B/Fluids*, Vol. 27, pp. 567-578.

Shirai, K., Büttner, L., Pfister, T., Czarske, J., Müller, H., Dopheide, D., Becker, S., Lienhart, H., and Durst, F., 2005, "High Spatially Resolved Turbulent Boundary Layer Measurements by Fiber-Optic Heterodyne-Velocity-Profile-Sensor", *Proc. 4th Int. Symp. on Turbulence and Shear Flow Phenomena (TSFP-4) Williamsburg, Virginia, USA, June 27-29, 2005*, pp.1219-1224.

Shirai, K., Bayer, C. Voigt, A., Pfister, T., Büttner, L., and Czarske, J., 2007, "Near-wall measurements of turbulence statistics with laser Doppler velocity profile sensors", *Proc. 5th Int. Symp. on Turbulence and Shear Flow Phenomena (TSFP-5), München, Germany, August 27-29, 2007*, pp. 279-284.

Tropea, C., Yarin, A., and Foss, J.F., 2007, "Handbook of Experimental Fluid Mechanics", Springer, Berlin.

Weier, T. Fey, U., Gerbeth, G., Mutschke, G., Lielausis, O., and Platacis, E., 2001, "Boundary layer control by means of wall parallel Lorentz forces", *Magnetohydrodynamics*, Vol. 37, pp. 177-186.

Weier, T., and Gerbeth, G., 2004, "Control of separated flows by time periodic Lorentz forces", *Euro. J. Mech., B/Fluids*, Vol. 23, pp. 835-849.

Weier, T., Cierpka, C., and Gerbeth, G., 2007, "Vortex structures in the separated flow on an inclined flat plate under electromagnetic forcing: influences of excitation wave form, frequency, and amplitude", *Proc. 5th Int. Symp. on Turbulence and Shear Flow Phenomena (TSFP-5), München, Germany August 27-29, 2007*, pp. 1105-1110.